

# Understanding the Calculations Behind the Vector Network Analyzer

Allison Duh

**Abstract**—The process of using a Short-Open-Load-Thru (SOLT) calibration kits to extract the scattering matrix parameters of an unknown device under test is explored with both a coaxial and an on-wafer device. The vector network analyzer is calibrated before taking measurements of the unknown device and/or de-embedding one device from another. Uncalibrated SOLT measurements of a device under test are then taken and used to calculate two different types of 2-port calibration error model (8 term and 12 term) and applied to uncalibrated S-parameters of a device under test to obtain the calibrated S-parameters and characterize the device.

**Index Terms**—Measurement standards, microwave measurement, calibration, measurement uncertainty

## I. INTRODUCTION

S-parameters are essential quantities in the microwave engineering world for understanding the behavior and characteristics of a device. Although today's vector network analyzers provide an easy, automated calibration process, it is important to understand what is happening inside the box. This paper documents exercises in shifting planes of calibrated measurement references, de-embedding devices, extracting S-parameters of both stand-alone components and on-wafer elements, and the computation of calibration error model terms for conversion of uncalibrated measurements to calibrated.

## II. PART 1

An unknown 2-port device is measured with three known termination calibration standards. By using reflection values calculated from the provided calibration kit in combination with the known reflection coefficients of the loads, the S-parameters of the device are extracted. Once the device is characterized, it is de-embedded from a cascade of two-port devices to find the S-parameters of the network with the device removed.

### A. Calibration of a Vector Network Analyzer

The calibration performed is a Short-Open-Thru-Load (SOLT) calibration using an 85052C 3.5mm kit. After calibrating the vector network analyzer, the calibration is then checked by reconnecting the kit standards. Across a wide frequency range of calibration, the measured reflection from open and short will have a phase shift at high frequencies due to the increasingly significant electrical length of the conductor line inside the calibration standard, also called the offset length. The validity of calibration magnitude and phase can be checked by recalculating the gamma reflection coefficients based off of the quantified electrical characteristics of the calibration kit and seeing if it matches the measured values. The gamma reflection coefficients are calculated using the following equations:

$$\Gamma_{open,calculated} = \Gamma_C \cdot \tau_{open,loss} \cdot \tau_{open,delay} \quad (1)$$

$$\Gamma_{short,calculated} = \Gamma_L \cdot \tau_{short,loss} \cdot \tau_{short,delay} \quad (2)$$

$$\Gamma_{load,calculated} = \Gamma_Z \cdot \tau_{load,loss} \cdot \tau_{load,delay} \quad (3)$$

where  $\Gamma_C$ ,  $\Gamma_L$ , and  $\Gamma_Z$  are the frequency-dependent reflection coefficients of the loads at the end of the conductor line inside the standard.  $\Gamma_C$  represents the open circuit,  $\Gamma_L$  the short and  $\Gamma_Z$  the fixed perfect termination load. The THRU standard determines the fourth relationship that

$$S_{21} = S_{12}$$

.Because the behavior of the capacitor and inductor changes with frequency (e.g. the capacitor radiates at high frequencies and increases the electrical length of the device), a third order polynomial model can be implemented for each of these values as follows [1]:

$$Z_c = C_0 + C_1 \cdot f + C_2 \cdot f^2 + C_3 \cdot f^3$$

$$Z_l = L_0 + L_1 \cdot f + L_2 \cdot f^2 + L_3 \cdot f^3$$

The values can be found in data sheets and parameters provided by the calibration kit manufacturers - for example,  $C_0 = 49.433E - 15F$ ,  $C_1 = -310.13E - 27F/Hz$ ,  $C_2 = 23.168E - 36F/Hz^2$  and  $C_3 = -0.15966E - 45F/Hz^3$  for this kit and  $L_0 = 2.0765E - 12H$ ,  $L_1 = -108.54E - 24H/Hz$ ,  $L_2 = 2.1705E - 33H/Hz^2$  and  $L_3 = -0.01E - 42H/Hz^3$ .

The  $\tau$  terms in Equations 1-3 reflect the loss and delay that arise from the offset length. The reference plane from which the measurements are taken is located at one end of the offset length and the calibration termination is located at the other. It follows transmission line theory that the reflection coefficient at the reference plane is that of the reflection coefficient calibration termination plane multiplied by the term  $e^{-2\gamma L}$ . This term can be broken down using  $\gamma = \alpha + j\beta$ .  $e^{-2j\beta d}$  becomes  $e^{-j4\pi f \tau}$  using the relationships  $v = f\lambda$  and  $\tau = \frac{d}{v}$  - this term represents the delay induced of the offset length. The loss due to metal conductivity of the offset length is proportional to the sheet resistance of resistance, a square-root relationship, and is defined as

$$\tau_{loss} = A\sqrt{f} = -\frac{\tau_{delay}}{Z_0}\sqrt{f}$$

where frequency is measured in gigahertz and

$$A = \frac{d\sqrt{\Delta L \Delta C}}{Z_0}$$

and

$$\tau_{delay} = d\sqrt{\Delta L \Delta C}$$

. More indepth discussion of the theory behind these measurements can be found in [1] and [2].

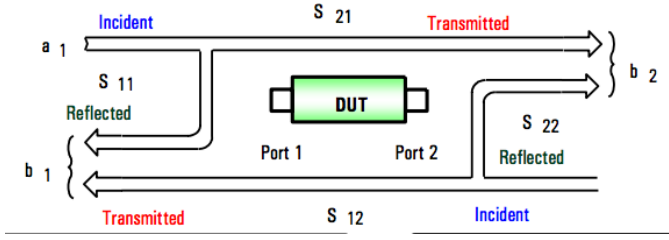


Fig. 1. The reflection coefficient looking to the right at port 2 can be related to the reflection coefficient looking to the right at port 1 by Equation 4.

### B. Extraction of 2-Port Coaxial S-Parameters

Using the calibrated VNA, the s-parameters of two different two-port devices will be extracted. The first is a 3.5-mm male-male barrel transition and the second is a filter.

The reflection coefficients at either port of a two-terminal device as shown in Figure 1 can be related to each other using the following equation [3]:

$$\Gamma_{in} = \frac{S_{11} - \Delta S \Gamma_{term}}{1 - S_{22} \Gamma_L} \quad (4)$$

where  $\Delta S = S_{11}S_{22} - S_{21}S_{12}$  and  $\Gamma_{term}$  is the reflection coefficient at the end of the offset length looking into a known standard.

If both reflection coefficients are known, as is the case here, the scattering matrix of the device under test can be obtained.

Three values of  $\Gamma_{in}$  have been measured at the reference plane:  $\Gamma_{short, meas}$ ,  $\Gamma_{open, meas}$  and  $\Gamma_{load, meas}$ . Three values of  $\Gamma_{term}$  have been calculated:  $\Gamma_{short, calc}$ ,  $\Gamma_{open, calc}$  and  $\Gamma_{load, calc}$ .

Using these three sets of measured and calculated gamma values, the three iterations of Eq. 4, can be reformed into three equations that define the terms  $S_{11}$ ,  $S_{22}$ , and  $S_{12}S_{21}$ .

$$S_{11} = \Gamma_{load, meas} \quad (5)$$

$$S_{22} = \frac{\Gamma_{short, calc} * (\Gamma_{open, meas} - \Gamma_{load, meas}) - \Gamma_{open, calc} * (\Gamma_{short, meas} - \Gamma_{load, meas})}{\Gamma_{open, calc} * \Gamma_{short, calc} * (\Gamma_{open, meas} - \Gamma_{short, meas})} \quad (6)$$

$$S_{12} = \pm \sqrt{\frac{(\Gamma_{open, meas} - \Gamma_{load, meas}) * (1 - S_{22} * \Gamma_{open, calc})}{\Gamma_{open, calc}}} \quad (7)$$

Once again, the THRU standard determines the fourth relationship that

$$S_{21} = S_{12}$$

The extracted scattering matrix parameters can be seen in Figures 2 and 3 – these parameters belong to a 3.5mm male-male barrel transition. It is important to note that Equation 7 has a plus-minus in its definition which affects the angle of this term. The proper sign must be chosen so that the calculated angle moves smoothly from  $+\pi$  to  $-\pi$  before jumping - if the incorrect sign is chosen the angle response will be erratic and cross the x-axis inaccurately.

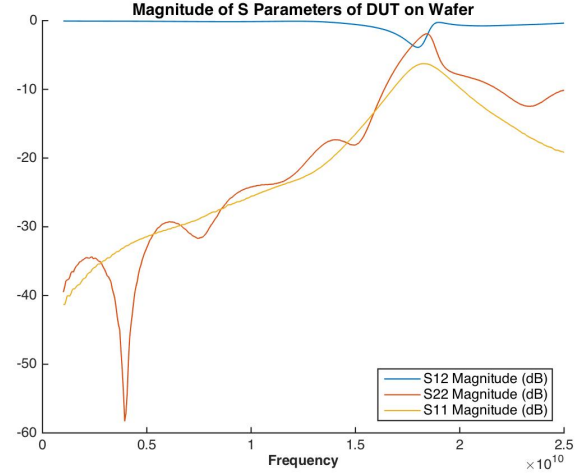


Fig. 2. The magnitude of the s parameters belonging to the extracted device.

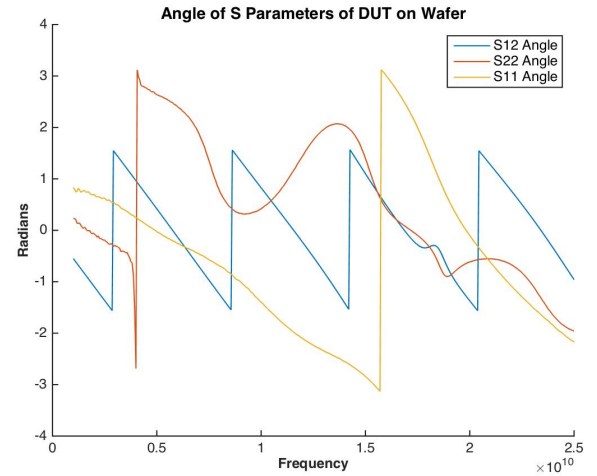


Fig. 3. Due to the square root taken in calculating the S21 parameter, care must be taken that the proper sign (plus or minus) is chosen so that the calculated angle moves smoothly from  $+\pi$  to  $-\pi$ .

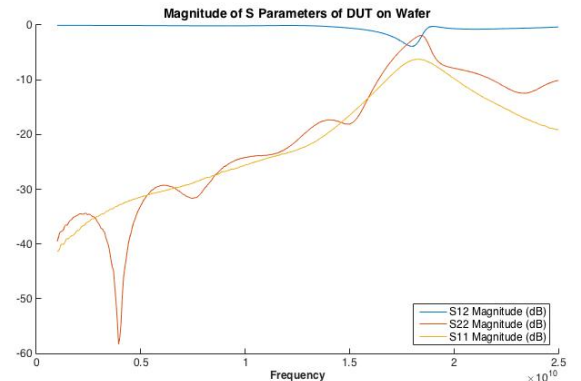


Fig. 4. The magnitude of the S parameters of the on-wafer device.

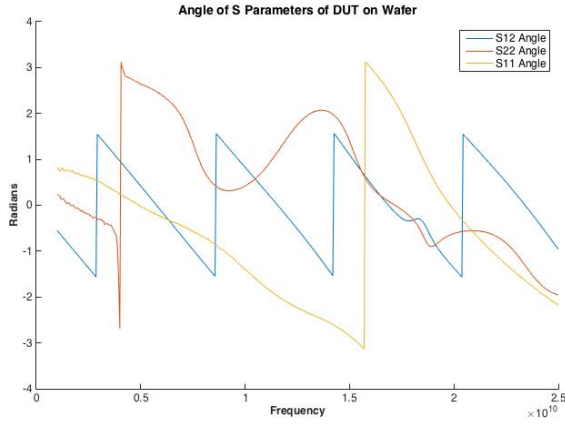


Fig. 5. The angle of the S-parameters of the on-wafer device.

### C. Extraction of 2-Port On-Wafer Device S-Parameters

The same SOLT extraction can also be carried out for an on-wafer device using a GSG and an on-wafer calibration kit. The calibration kit parameters used were as follows:

- $C_0 = -7E - 15F$
- $C_1 = 0F/Hz$
- $C_2 = 0F/Hz^2$
- $C_3 = 0F/Hz^3$
- $L_0 = 18.20E - 12H$
- $L_1 = 0H/Hz$
- $L_2 = 0H/Hz^2$
- $L_3 = 0H/Hz^3$
- Delay=0ps (for all cases)
- Loss=0 Ohm/s (for all cases)
- $Z_0=50$  (for all cases)

and the extracted parameters can be seen in Figures 4 and 5.

### D. De-embedding of Device and 2-Port Coaxial Extraction

The next device whose scattering parameters need to be extracted is a filter that is connected to the previously extracted 3.5mm transition. The measurement is taken from one end of the transition to the other end of the filter. In order to extract the S-parameters of the filter, scattering transfer parameters, or T-parameters, can be used. Whereas the scattering matrix is defined as

$$\begin{pmatrix} b_1 \\ b_2 \end{pmatrix} = \begin{pmatrix} S_{11} & S_{12} \\ S_{21} & S_{22} \end{pmatrix} \begin{pmatrix} a_1 \\ a_2 \end{pmatrix},$$

the scattering transfer parameters are defined as follows:

$$\begin{pmatrix} a_1 \\ b_1 \end{pmatrix} = \begin{pmatrix} T_{11} & T_{12} \\ T_{21} & T_{22} \end{pmatrix} \begin{pmatrix} b_2 \\ a_2 \end{pmatrix}.$$

T-parameters relate incident and reflected waves at each port. The conversion equations between S and T-parameters can be found in many standard microwave textbooks such as [4]. T-parameters lend themselves more easily than S-parameters to calculating the incident and reflected waves at

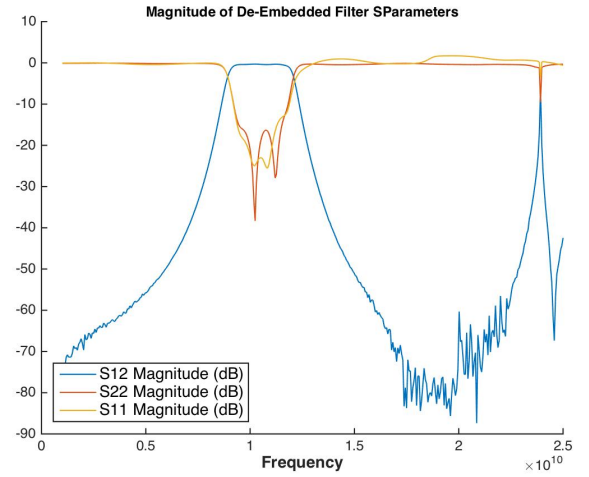


Fig. 6. The magnitude of the filter S-parameters calculated from the T-matrix conversion. Erratic behavior begins around 14GHz.

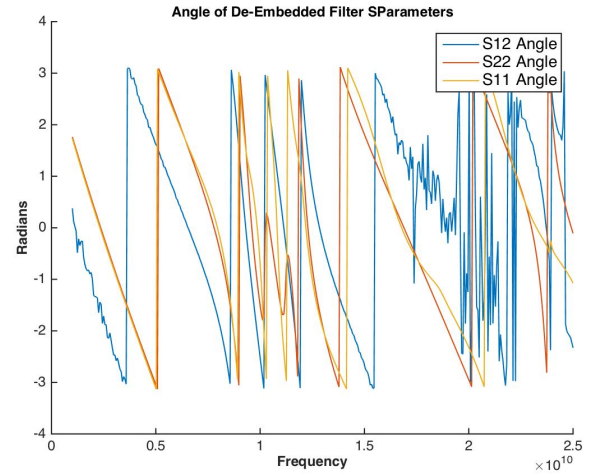


Fig. 7. The phase of the filter S-parameters calculated from the T-matrix conversion. Noticeable erratic behavior begins around 16GHz.

the input and output of a system of cascaded devices. In this case,

$$[T_{total}] = [T_{transition}][T_{filter}] \quad (8)$$

$$[T_{transition}]^{-1}[T_{total}] = [T_{filter}] \quad (9)$$

Using the calibrated VNA S-parameter measurements and the computed S-parameters of the transition converted to T-matrices, the T-matrix of the filter can be computed and then be converted back into S-parameters, the magnitude and angle of which are shown in Figures 6 and 7.

The filter's response is centered around 10.5 GHz with a 3dB bandwidth of 3.4GHz. The magnitude of the  $S_{11}$  response becomes greater than 0dB around 14 GHz, and the magnitude and angle response of  $S_{12}$  become erratic around 17 GHz. Furthermore there is a slight resonance around 24 GHz. One possible explanation for this is that the filter is not

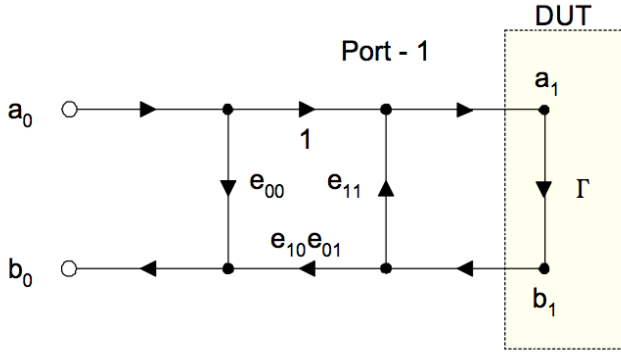


Fig. 8. The signal flow graph relating the error terms of a one-port device.

designed to be measured at such high frequencies and thus its measurements display irregularities and unexpected behavior.

### III. PART II

In Part I the vector network analyzer was calibrated before taking measurements of the unknown device and/or de-embedding one device from another. It is also possible to take uncalibrated measurements of a device under test using three known terminations and a through measurement to and calculated error terms which then can be applied to uncalibrated S-parameters of a device under test to obtain the calibrated S-parameters. There are several error models that can be applied to measurements, depending on the type of network analyzer being used, such as the 12-term error model, the 8-term error model and the 16-term error model. In this paper, the 12-term and 8-term models will be explored.

#### A. 12-term model

The 12 term model is used for incomplete reflectometers, which are often older and lower-cost. Incomplete means that the VNA has only 3 receivers rather than 4, and of the four waves ( $a_1, b_1, a_2, b_2$ ) only  $a_1$  or  $a_2$  can be measured, with a forward or backward mode measurement, respectively, at the same time as  $b_1$  and  $b_2$ . The forward mode measurement uses the raw  $S_{11}$  and  $S_{21}$  measurements, and the reverse mode uses the raw  $S_{22}$  and  $S_{12}$ . For each mode, there is a corresponding one-port model (Fig. 8) that provides for 3 of the required 6 error terms per mode – the calculations of the calibration standard reflection coefficients from Part 1 can be used again.

$$\begin{pmatrix} \Gamma_{S,meas} \\ \Gamma_{O,meas} \\ \Gamma_{L,meas} \end{pmatrix} = \begin{pmatrix} 1 & \Gamma_{S,meas}\Gamma_{S,calc} & \Gamma_{S,calc} \\ 1 & \Gamma_{O,meas}\Gamma_{O,calc} & \Gamma_{O,calc} \\ 1 & \Gamma_{L,meas}\Gamma_{L,calc} & \Gamma_{L,calc} \end{pmatrix} \begin{pmatrix} e_{00} \\ e_{11} \\ \Delta_E \end{pmatrix}$$

where  $\Delta_E = e_{00}e_{11} - e_{10}e_{01}$ .

The three remaining terms of the forward-mode are  $e_{30}$ ,  $e_{22}$  and  $e_{10}e_{32}$ . The  $e_{30}$  term is related to isolation and it can be assumed that the ideal isolated S parameter matrix is a 2x2 zero matrix; thus

$$e_{30} = S_{21,measured}$$

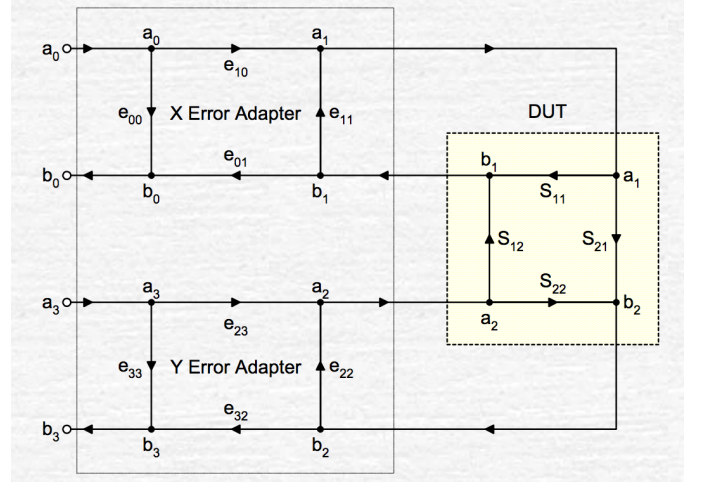


Fig. 9. The signal flow graph of the 8-term model.

. The through standard connects the two ports together and has an S matrix ideally of

$$\begin{pmatrix} 0 & 1 \\ 1 & 0 \end{pmatrix}$$

The latter two terms are based off of this through standard as follows

$$e_{22} = \frac{S_{11,m} - e_{00}}{S_{11,m}e_{11} - \Delta_e}$$

$$e_{10}e_{32} = (S_{21,m} - e_{30})(1 - e_{11}e_{22})$$

With the reverse mode, the same terms can be calculated in the same manner. The one-port terms in the reverse directions are  $e'_{33}$ ,  $e'_{22}$  and  $e'_{23}e'_{32}$ . The remaining isolation and thru terms are  $e'_{03}$ , and  $e'_{11}$  and  $e'_{23}e'_{01}$ , respectively. With all twelve terms calculated, the calibrated data can now be computed using the uncalibrated measurements as follows:

$$D = \left(1 + \frac{(S_{11,m} - e_{00})}{e_{10}e_{01}}e_{11}\right) \left(1 + e'_{22} \frac{S_{22,m} - e'_{33}}{e'_{23}e'_{32}}\right) - \left(\frac{S_{21,m} - e_{30}}{e_{10}e_{32}}\right) \left(\frac{S_{12,m} - e'_{03}}{e'_{23}e'_{01}}\right) e_{22}e'_{11}$$

$$S_{11} = \frac{\left(\frac{S_{11,m} - e_{00}}{e_{10}e_{01}}\right) \left(1 + \frac{S_{22,m} - e'_{33}}{e'_{23}e'_{32}}e'_{22}\right) - e_{22} \left(\frac{S_{21,m} - e_{30}}{e_{10}e_{32}}\right) \left(\frac{S_{12,m} - e'_{03}}{e'_{23}e'_{01}}\right)}{D}$$

$$S_{21} = \frac{\left(\frac{S_{21,m} - e_{30}}{e_{10}e_{32}}\right) \left(1 + \left(\frac{S_{22,m} - e'_{33}}{e'_{23}e'_{32}}\right)(e'_{22} - e_{22})\right)}{D}$$

$$S_{22} = \frac{\left(\frac{S_{22,m} - e'_{33}}{e'_{23}e'_{32}}\right) \left(1 + \frac{S_{11,m} - e_{00}}{e_{01}e_{10}}e_{11}\right) - e'_{11} \left(\frac{S_{21,m} - e_{30}}{e_{10}e_{32}}\right) \left(\frac{S_{12,m} - e'_{03}}{e'_{23}e'_{01}}\right)}{D}$$

$$S_{12} = \frac{\left(\frac{S_{12,m} - e'_{03}}{e'_{23}e'_{01}}\right) \left(1 + \left(\frac{S_{11,m} - e_{00}}{e_{01}e_{10}}\right)(e_{11} - e'_{11})\right)}{D}$$

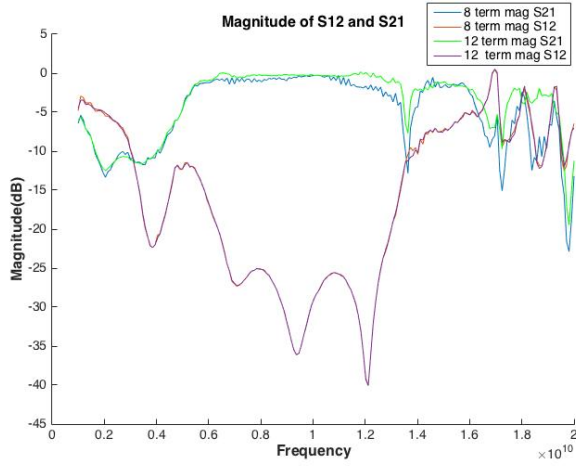


Fig. 10. The magnitude of the S21 calculated by the 8 and 12 terms become less aligned after 12 GHz. S22 is strongly correlated between the methods.

### B. 8-term model

The eight-term model is used with a complete reflectometer which has four receivers and can measure both incident and reflected waves simultaneously. The signal flow graph of the 8-term model can be seen in Figure 9. The X, DUT and Y networks are cascaded to yield the collected measured values,

$$[T_m] = [T_X][T_{DUT}][T_Y]$$

The T-parameters of the X and Y networks can be expressed in terms of the signal flow graph values from the two one-port forward and reverse mode calibrations.

$$[T_X] = \frac{1}{e_{10}} \begin{bmatrix} 1 & -e_{11} \\ e_{00} & -\Delta X \end{bmatrix}$$

where  $\Delta X = e_{00}e_{11} - e_{10}e_{01}$

$$[T_Y] = \frac{1}{e_{32}} \begin{bmatrix} 1 & -e_{33} \\ e_{22} & -\Delta Y \end{bmatrix}$$

where  $\Delta Y = e_{22}e_{33} - e_{32}e_{23}$

Instead of solving for two more terms, a normalized 7th term can be used to complete the error terms for the 8-term model. This term is  $e_{10}e_{32}$  and it is computed from the through calibration measurement. A further discussion of the error term models can be found in [5].

$$e_{10}e_{32} = [T_m]^{-1}[A][T_{DUT}][B] \quad (10)$$

where

$$[T_{DUT}] = \begin{bmatrix} 0 & 1 \\ 1 & 0 \end{bmatrix}$$

In practice, the left side of Equation 10 will evaluate out to a 2-x-2 matrix of unique values rather than one identical value. The value of the first row and the first column was chosen in calculating the  $T_{DUT}$  parameters. Choosing this value is successful in preventing the erratic jumps in phase seen in the previous section.

Figures 10-13 display the magnitude and phase of the calibrated data and discuss the qualitative differences in the magnitude and phases computed by using the two different

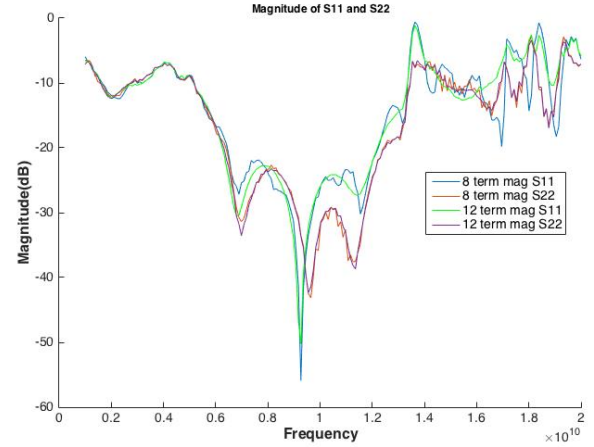


Fig. 11. The magnitudes of the S11 calculated by the 8 and 12 terms follow roughly the same shape but the 12 term graph is smoother after the 10 GHz mark and takes less dips in magnitude than the 8 term calculation. S22 is strongly correlated between the methods.

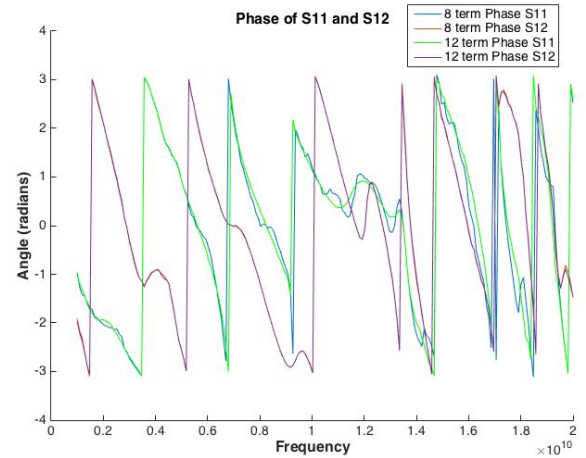


Fig. 12. The 12 term calculation of S11 phase is smoother and less erratic in shape than the 8-term calculation, especially after the 10GHz mark. The two S12 phases is strongly correlated.

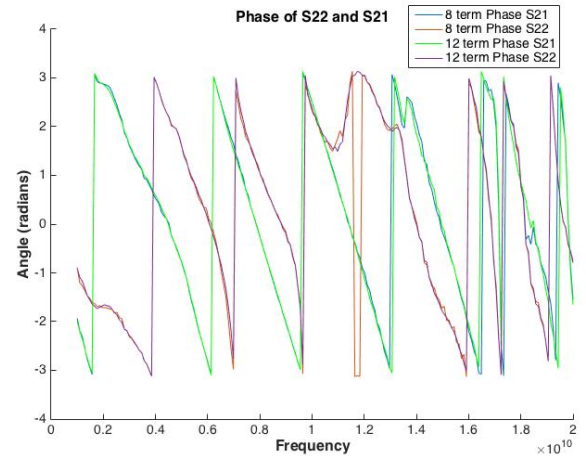


Fig. 13. Except for a dip around 12 GHz in the 12-term calculation of the S22 phase, the two methods of calculation compute phases for S21 and S22 which are very strongly correlated.

error models. The device under test is an isolator centered at 9.5GHz with a 3dB bandwidth of 7 GHz, because the  $S_{21}$  is close to 0dB and the  $S_{12}$  less than -20 dB from 6 to 13 GHz.

#### IV. CONCLUSION

The various s-parameters computed in this paper demonstrate that magnitude error is often smaller and more predictable than phase error. The phase response of a passive device is linear and should ideally move smoothly from  $+\pi$  to  $-\pi$ ; however the  $j$  term that is often involved in phase computation means that the phase response will often be erratic if not computed properly.

Furthermore, the versatility of the signal flow/S parameter-T parameter relationship is strongly demonstrated in characterizing de-embedded and cascaded devices and networks. The signal flow graph is useful in relating the incident and reflected waves of a network amongst themselves, but the T-parameter rearranges them to be easily used in to relate the behavior of a network to the behavior of its individual components.

#### REFERENCES

- [1] Agilent, "Specifying Calibration Standards and Kits for Agilent Vector Network Analyzers," Appl. Note 1287-11.
- [2] D. C. DeGroot, K. L. Reed and J. A. Jargon, "Equivalent Circuit Models for Coaxial OSLT Standards," ARFTG Conference Digest-Spring, 54th, Atlanta, GA, USA, 1999, pp. 1-13.
- [3] Agilent, "Specifying Calibration Standards and Kits for Agilent Vector Network Analyzers," Appl. Note 1287-11.
- [4] D. M. Pozar, Microwave Engineering, 2nd ed. New York: Wiley, 1998.
- [5] D. Rytting, Network analyzer error models and calibration methods. September 1998, Hewlett-Packard Company